

## RETRACTED

### Effects of N-acetylcysteine and metformin treatment on the stereo-pathological characteristics of uterus and ovary

Bahare Rafiee (1), Saied Karbalay-doust (2), Seyed Mohammad Bagher Tabei (3), Negar Azarpira (4), Sanaz Alaei (5), Parvin Lohrasbi (6), Soghra Bahmanpour (7)

(1) Department of Reproductive Biology, School of Advanced Medical Sciences and Technologies, Shiraz University of Medical Sciences, Shiraz, Iran; (2) Histomorphometry and Stereology Research Center, Department of Anatomy, School of Medicine, Shiraz University of Medical Sciences, Shiraz, Iran; (3) Maternal-Fetal Medicine Research Center, Department of Medical Genetics, School of Medicine, Shiraz University of Medical Sciences, Shiraz, Iran; (4) Transplant Research Center, Shiraz University of Medical Sciences, Shiraz, Iran; (5) Department of Reproductive Biology, School of Advanced Medical Sciences and Technologies, Shiraz University of Medical Sciences, Shiraz, Iran; (6) Department of Reproductive Biology, School of Advanced Medical Sciences and Technologies, Shiraz University of Medical Sciences, Shiraz, Iran; (7) School of Medicine, Shiraz University of Medical Sciences, Shiraz, Iran.

This article is distributed under the terms of the Creative Commons Attribution Noncommercial License (CC BY-NC 4.0) which permits any noncommercial use, distribution, and reproduction in any medium, provided the original author(s) and source are credited.

#### Abstract

In this study, the stereo-pathological effect of metformin and N-acetyl cysteine is evaluated on the uterus and ovary of polycystic ovary syndrome (PCOS) mice. 96 mature females (8-week-old, weight of 20–30 gr) BALB/c mice were classified into 6 groups including the control group (n= 16), letrozole-induced PCOS group (n=16), PCOS + metformin (n=16), PCOS+NAC (n=16) and a separate control group for NAC (n=16). Another PCOS group was maintained for a month to make sure that features remain till the end of the study. Testosterone level, vaginal cytology and stereological evaluations were assessed. Vaginal cytology in letrozole-receiving mice showed a diestrus phase continuity. Testosterone level, body weight, uterine weight, endometrial volume, myometrial volume, gland volume, stromal volume, epithelial volume, vessel volume, daughter and conglomerate glands, endometrial thickness, and myometrial thickness exhibited an increasing trend in the uterus of PCOS mice. While normal gland and vessel length decreased in the PCOS group. Ovarian volume, corticomedullary volume, primary follicles, secondary follicles, and ovarian cysts were increased in PCOS ovaries. While corpus luteum, primordial, graafian, and atretic follicles showed a decline in the PCOS group. NAC and metformin, however, managed to restore the condition to normal. Given the prevalence of PCOS and its impact on fertility, the use of non-invasive methods is of crucial significance. NAC can control and treat pathological parameters and help as a harmless drug in the treatment of women with PCOS.

**Key Words:** Polycystic ovary syndrome (PCOS); metformin; N acetylcysteine; stereology; pathology.

Eur J Transl Myol 32 (2): 10409, 2022 doi: 10.4081/ejtm.2022.10409

Polycystic ovary syndrome (PCOS) is a common hormonal disorder in reproductive age. According to Rotterdam criteria, this syndrome can be diagnosed by two of the three symptoms of clinical/biochemical hyperandrogenism, ovarian dysfunction, and the presence of 12 or more follicles of 2-10 mm in the ovary.<sup>1</sup> Although the number of oocytes retrieved in PCOS is higher than the others, most of them are not

mature, declining the pregnancy rate.<sup>2</sup> Oocyte, embryo quality, and pregnancy outcomes are weaker in PCOS patients due to changes in the oocyte and follicular fluid microenvironment.<sup>3</sup> Pathological variations of ovaries and uterus in PCOS are the most important causes of ART failure. Uterine exposure with high levels of free insulin, growth factor-I, and androgens, increases endometrial proliferative activity, and endometrial thickness.<sup>4</sup> The incidence of micropolyp is also

associated with endometritis (plasma cells infiltration into endometrial stroma), endometrial stromal edema, and peri-glandular hyperemia.<sup>5</sup> In the ovary, the presence of cystic follicles with a thin layer of granulosa cells and the absence of corpus luteum (indicative of anovulation status) is a common finding.<sup>6</sup> One of the most basic treatment lines of PCOS is metformin. Metformin is a biguanide used to treat hyperglycemia, reduce insulin resistance, and inhibit hepatic gluconeogenesis. It also reduces total and free blood androgen, corrects ovarian dysfunction, and increases the quality of oocyte and embryos by reducing ROS and apoptosis levels.<sup>7</sup> Metformin consumption in PCOS patients can decline premature and pre-antral follicles.<sup>8</sup> Metformin consumption can also enhance follicular development, improve the percentage of corpus luteum, and decrease cystic follicles, hence, facilitating ovulation and fertility rate.<sup>9</sup> Metformin also increments endometrial receptivity markers in PCOS patients.<sup>10</sup> Metformin is, however, associated with gastrointestinal side effects. Another treatment that may help reduce PCOS complications and ultimately increase the chances of fertility is N-Acetyl cysteine (NAC). NAC is a derivative of the amino acid cysteine with antioxidant effects. Its anti-apoptotic properties prevent ovarian ischemia. NAC consumption is associated with a decrease in testosterone. Therefore, NAC can have positive effects on ovulation in PCOS patients.<sup>11</sup> NAC can effectively strengthen pregnancy and ovulation rates. It is safe with a high lethal dose threshold, resulting in no side effects. However, the underlying mechanism of how NAC administration protects the utero-ovarian function (that reverse histopathological characteristics in PCOS) still needs further exploration.<sup>12-28</sup> In this regard, the present study is aimed to evaluate the stereo pathological effects of metformin and N-acetyl cysteine on uterus and ovary in letrozole-induced PCOS mice to find probable mechanisms.

## Materials and Methods

### *Ethics statement*

All experiments on the animals in this study were approved by the Animal Ethical Committee of Shiraz University of Sciences (IR.SUMS.REC.1398.620).

### *Animal maintenance and treatment*

96 mature females (8-week-old, weight of 20-30 gr) BALB/c mice were purchased from Comparative and Experimental Medical Center of Shiraz University of Medical Sciences. The animals were kept for two weeks to adapt to the environment. All experiments were conducted between 9:00 a.m. to 12:00 p.m. under standard laboratory conditions ( $22 \pm 2^\circ\text{C}$  room temperature; 12-h light/dark cycle with lights on at 7:00 a.m.). Tap water and food pellets were provided ad libitum. Female mice were randomly divided into 6 groups (n=16) as follows. PCOS group: To induce

PCOS, mice received letrozole (Letrax 2.5, Abu Raihan pharmaceutical Co, Tehran, Iran) at a dose of 90  $\mu\text{g}/\text{kg}$  daily for one week by gavage. The effective dose for induction of PCOS in the mice model was determined by experimenting with 60, 90, 120, and 200  $\mu\text{g}/\text{kg}$  daily doses for a week, on 4 groups of 8 mice as a pilot study. After measuring the necessary criteria such as vaginal cytology, serum testosterone levels, and weight, the dosage of 90  $\mu\text{g}/\text{kg}$  daily was selected. Metformin-treated group: PCOS mice received metformin (metformin 500, Fagher Co, Tehran, Iran) at 500 mg/kg daily by gavage for 7 days.<sup>12</sup> Control group: Animals received distilled water (as letrozole and metformin solvent) by gavage daily. NAC treatment group: For 9 days, mice with PCOS received NAC (N-acetyl cysteine, Sigma-Aldrich, product number A7250) at a dose of 160 mg/kg dissolved in 0.9% NaCl by intraperitoneal injection. The effective dose of NAC for PCOS treatment in mice was first determined by testing various doses (90, 150, 160, and 200 mg/kg per day) for a week, on 4 groups of 8 mice as a pilot study. After measuring the necessary criteria such as vaginal cytology, serum testosterone levels, and weight the dosage of 160  $\mu\text{g}/\text{kg}$  daily was selected. NAC Control group: Mice received 0.9% NaCl by intraperitoneal injection for 9 days. PCOS group: PCOS mice in this group were kept for 4 weeks without any therapeutic intervention to ensure the durability of PCOS features till the end of the study

### *Estrous cycle determination and vaginal cytology*

Daily vaginal smears were taken between 9 to 10 in the morning. The stages of the sexual cycle were determined based on vaginal cytology. Vaginal cells were collected by lavage of distilled water, fixed on a slide, and stained by Giemsa.<sup>13</sup>

### *PCOS induction proofs*

The weight of the rats was measured weekly, estrus cycle was determined daily, serum testosterone levels were measured. Finally, a stereological study was performed of the right ovary and uterine horn.

### *Serum testosterone*

After blood sampling and isolation of serum, the samples were frozen at  $-80^\circ\text{C}$ . The testosterone level was then evaluated by the ELISA method using a special kit (kit range of 10-800 ng /dl) according to the manufacturer's instructions.

### *Stereological study*

Preparation of the uterine tissue

At the end of the studies, the mice were sacrificed. Through a midline incision, the ovaries and uterus were exposed, cleaned, and removed. (Figure 1 a). The right and left uterine horns were cut from the uterine tube and vagina (Figure 1 b). After measuring the weight of the uterine horns, their volume, V(uterine horns), was measured by the immersion technique. Subsequently, 8

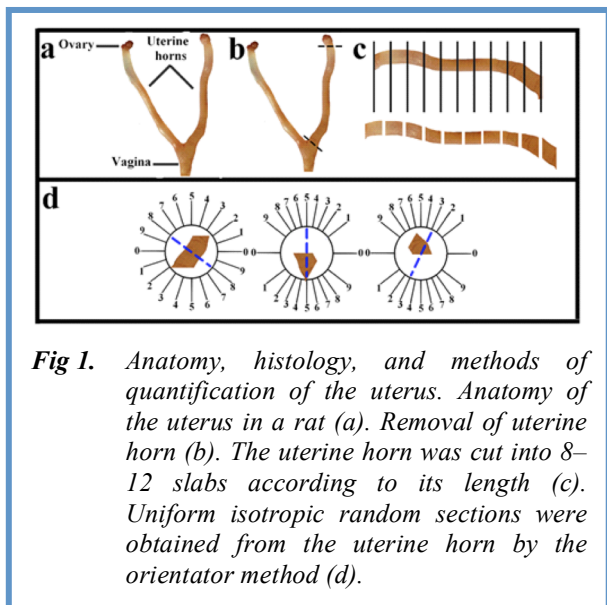


**Fig 1.** Anatomy, histology, and methods of quantification of the uterus. Anatomy of the uterus in a rat (a). Removal of uterine horn (b). The uterine horn was cut into 8–12 slabs according to its length (c). Uniform isotropic random sections were obtained from the uterine horn by the orientator method (d).

to 12 parallel sections were obtained based on the length of the uterine horn (Figure 1 c). To estimate the total length of the vessels, the parts of the left uterine horn were cut using isotropic uniform random (IUR) sections procedure (Figure 1).<sup>14,15</sup> Each uterine horn segment was sectioned into pieces parallel to the direction of the second cut with a distance of 1 mm, giving rise to 8-12 slabs. The slabs were then held in 10% neutral buffered formalin for tissue procedure. The slabs were processed, embedded into separate paraffin blocks, sectioned (4 and 25 μm thickness), and stained with Hematoxylin and Eosin (H&E).

#### Estimating the volumes of the uterine wall components

The four-micron-thick sections of the right uterine horn were used to investigate the volume of the perimetrium, myometrium, and endometrium (epithelium, gland, stroma, and blood vessels) layers of the uterine horn (Figure 2). The stereological instrument included a Nikon E-200 microscope (Tokyo, Japan) with an oil objective lens (Plan Apo 60x, n/a: 1.4, Tokyo, Japan) and a Samsung video camera (SCB- 2000P, Hanwha Techwin, South Korea) attached to a computer. The stereological probes at the final magnification of 385 X

were applied to the live image and the volume of listed structures was estimated by the “point counting method”. The volume density of uterine structures,  $V_v$  (structure) was calculated by the following formula:

$$V_v (\text{structure}) = \Sigma P (\text{structure}) / \Sigma P (\text{total}).$$

In which  $\Sigma P$  (structure) and  $\Sigma P$  (total) are the total points that fall on the structures of the uterus and the total points that fall on the uterine section, respectively. The total volume of the uterine structures was assessed by multiplying the volume density ( $V_v$ ) by V (uterine horn).

#### Estimating the number of uterine glands

The optical dissector technique was applied to estimate the number of uterine glands. The optical dissector is composed of an Eclipse microscope (E200, Nikon, Tokyo, Japan) with a high numerical aperture (NA=1.30) ×40 oil-immersion objective, attached to a video camera, to project the live image to a monitor, and an electronic microcator with digital readout (MT12, Heidnehain, Traunreut, Germany) for assessing the movements in the Z-axis with an accuracy of 0.5μm. The location of microscopic fields was determined, by moving the microscopic stage in x- and y-axes at equal distances with systematic uniform random sampling. The unbiased counting frame is a 3D probe used to count the number of the uterine gland, with a stereology software system (Stereolite, SUMS, Shiraz, Iran). The counting frame has two solid forbidden lines (the left and inferior borders and their extensions) and two dashed acceptance lines (the right and superior borders) that were superimposed on the live image uterus at a final magnification of 10 X (Figure 2c). The guard zone refers to areas at the top and bottom parts of the uterine sections. These areas were used to avoid cutting tissue artifacts that take place during tissue procedures on this area of the uterine sections. Glands occurring in the focus zone above (the first 3.5 μm) or below (the first 3.5 μm) guard zones were not counted. The middle distance between the guard zones was the “height of the dissector” (here, 18 μm).<sup>16</sup> The uterine glands appeared in the maximal focus in the counting frame which were totally or partially placed in the frame and did not touch the solid line were selected.

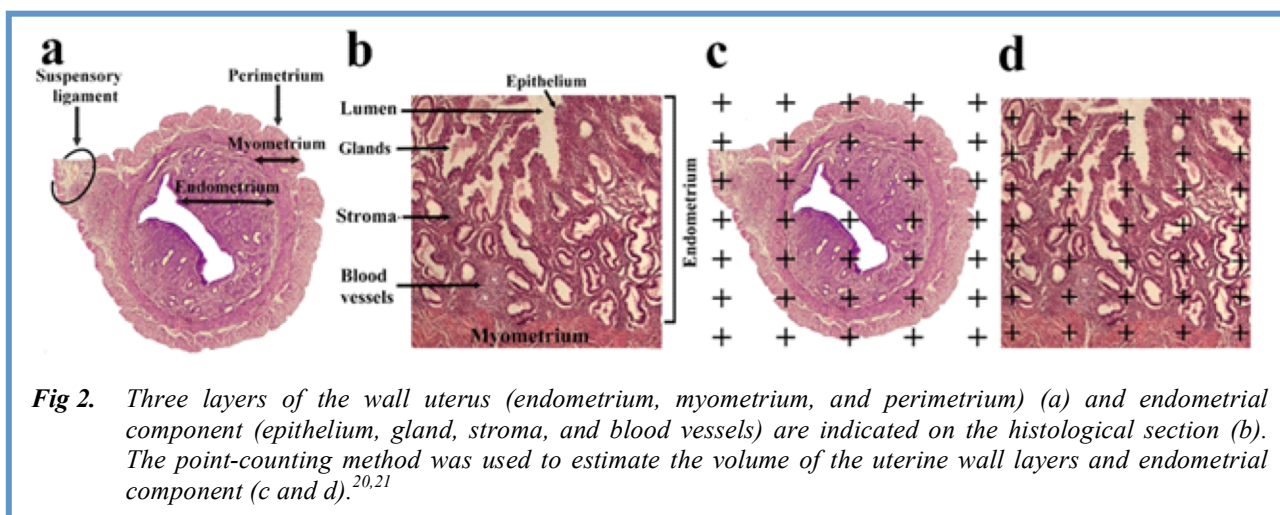


**Fig 2.** Three layers of the wall uterus (endometrium, myometrium, and perimetrium) (a) and endometrial component (epithelium, gland, stroma, and blood vessels) are indicated on the histological section (b). The point-counting method was used to estimate the volume of the uterine wall layers and endometrial component (c and d).<sup>20,21</sup>

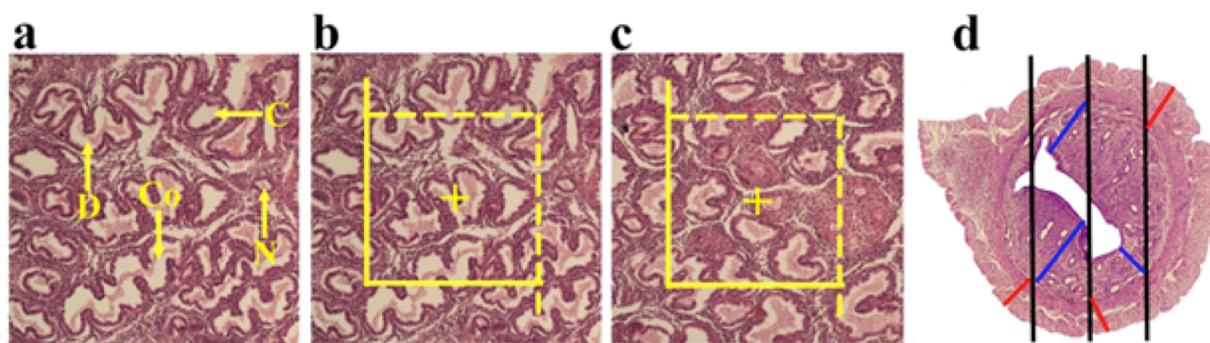


**Fig 3.** Methods of quantification of the uterus. The conglomerate (Co), cystic (C), daughter (D) and normal (N) morphological types of endometrial glands are indicated on the histological section (a). The optical disector method was applied to estimate the number of the endometrial glands (b). Estimation of the length of the blood vessels by unbiased counting frame (c). Estimation of the endometrial and myometrial thickness by orthogonal intercept method (d).<sup>20,2</sup>

The numerical density of the gland was estimated by the following equation:

$$N_v (\text{glands} / \text{total}) = \Sigma Q^- / (\Sigma P \times (a/f) \times h) \times (t/BA)$$

Where  $\Sigma Q^-$  is the number of the glands coming into in dissector height,  $\Sigma P$  shows the total of the counting frames in all microscopic fields, and  $h$  indicates the height of dissector.  $a/f$  also denotes the area of the frame.  $t$  and  $BA$  are the actual section thickness calculated with the microcator and the block advance of the microtome. The thickness of the uterine section was measured in the total microscopic fields considering uniform random sampling of each uterine section.<sup>17</sup>

The total number of the glands was assessed by multiplying the numerical density by  $V$  (uterine horn)<sup>17</sup>.

#### Morphology of the endometrial gland

For morphological assessment of endometrial glands, the video-microscopy system was used and the slides with a thickness of  $4 \mu\text{m}$  were evaluated at a final magnification of  $\times 400$ .<sup>18</sup> Finally, the percentage of the mentioned glands was estimated as the number of a normal, cystic, daughter, and conglomerate gland  $\times 100$  / total number of the gland (Figure 2).

#### Estimating the endometrial and myometrial thickness

To estimate the mean thickness of the mentioned structures of the uterus, the harmonic mean thickness of the listed structures was estimated. The sections with a thickness of  $4 \mu\text{m}$  were applied to evaluate the thickness. The stereological probe (isotropic lines) at the final magnification of  $10 \times$  was superimposed on the live images of the uterus and the distance between the internal and external surfaces of the listed structure was measured by drawing a vertical line from the external surface to the touchpoint of the isotropic line with the internal surface of the mentioned structure (Figure 3).<sup>19</sup> The mean thickness of the structures was then estimated by:

$$\text{Harmonic mean layer thickness} = 8 / (3\pi) \times \text{harmonic mean of orthogonal intercepts}$$

In this formula, the harmonic means of orthogonal intercepts = number of measurements/sums of the reciprocal of orthogonal intercepts ( $o_i$ )

$$\text{Number of measurements} / [1/o_i + 1/o_i + 1/o_i + 1/o_i + \dots]$$

#### Estimation of the length of the uterine blood vessels

The length density of the uterine vessels was determined using the four-micron-thick sections followed by an assessment with an unbiased counting frame (Figure 3). The unbiased counting frame with solid forbidden and dashed acceptance lines was overlaid on the live figures of the uterine horn tissue. The vessels entirely or partially residing in the unbiased counting frame which do not touch the solid forbidden lines were counted.<sup>14</sup> The length density of the vessels ( $LV$ ) was estimated by the following formula:

$$LV (\text{blood vessels} / \text{uterus}) = 2 \Sigma Q / (\Sigma P \times a/f)$$

where  $\Sigma Q$  is the whole number of the blood vessels whose diameter was above  $20 \mu\text{m}$ , sampled by the unbiased counting frame per rat uterus,  $\Sigma P$  also represents the number of frames associated points hitting the uterine tissue, and  $a/f$  shows the counting frame area. The total length of blood vessels  $L$  (vessels) was determined by the following formula:

$$L (\text{blood vessels}) = LV (\text{vessels} / \text{uterus}) \times V (\text{uterine horn})$$

#### Preparation of the ovary tissue section

After measuring the weight of the right ovary, it was processed and embedded in cylindrical paraffin blocks followed by cutting based on serial sections. Isotropic uniform random (IUR) sections with thicknesses of  $4$  and  $25 \mu\text{m}$  were obtained by a microtome and stained with H&E.

#### Estimation of the ovary volume

The Cavalieri technique was used to assess the total volume of the ovary at the final magnification of  $40 \times$

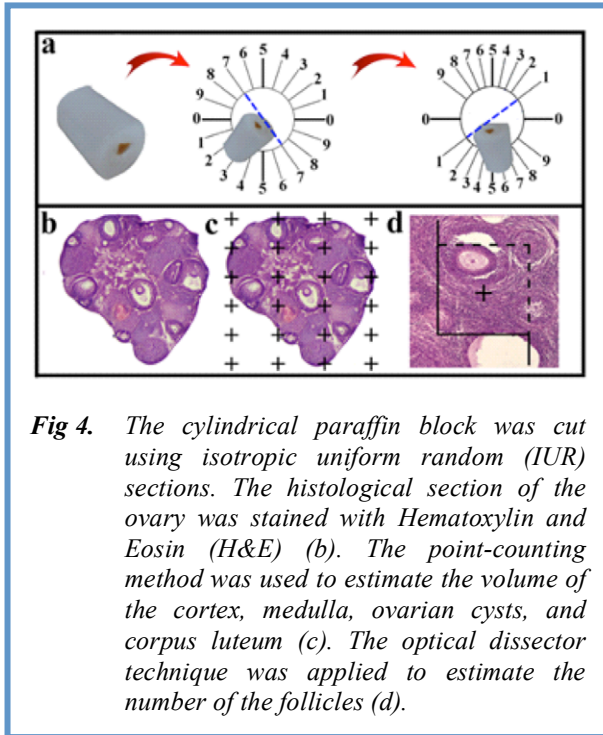


**Fig 4.** The cylindrical paraffin block was cut using isotropic uniform random (IUR) sections. The histological section of the ovary was stained with Hematoxylin and Eosin (H&E) (b). The point-counting method was used to estimate the volume of the cortex, medulla, ovarian cysts, and corpus luteum (c). The optical dissector technique was applied to estimate the number of the follicles (d).

(Figure4). To this end, 8-12 sections were selected from each mouse by systematic random sampling. The volume of the ovary was evaluated by point-counting technique through the following formula:

$$V(\text{ovary}) = A \times T \quad A = \sum P(\text{ovary}) \times a/p$$

In this formula,  $\sum P$  is the total number of points superimposed on the live images of the ovary,  $a/p$  shows the area related to each point, and  $T$  denotes the distance between the selected sections.

Estimation of the volume of cortex, medulla

The section with a thickness of 4  $\mu\text{m}$  was applied to evaluate the volume density of the structures. In every section, the cortex, medulla, ovarian cysts, blood vessels, and corpus luteum were identified (Figure 4). The stereological probes at the final magnification of 52 $\times$  were also used to the images and the volume density ( $V_v$  (structure/total)) of the listed structures were estimated by the point-counting method (Figure 4) and the following formula:

$$V_v(\text{structure}) = \frac{\sum P(\text{structure})}{\sum P(\text{total})}$$

In which  $\sum P(\text{structure})$  and  $\sum P(\text{total})$  are the total points superimposed in the chosen structure and the total points hitting the ovary sections, respectively. Finally, the total volume of each structure can be assessed by multiplying the volume density by  $V(\text{ovary})$

$$V(\text{structure}) = V_v(\text{structure}) \times V(\text{ovary})$$

Estimation of the number of Primordial, Primary, Secondary, Graafian, Atretic follicles and corpus luteum

The number of primary, secondary (antral), mature (Graafian), and atretic oocytes and granulosa cells was estimated by evaluating 25-micron-thick sections by

optical dissector method as described earlier. The number of follicles subpopulations can be assessed by the following formula:

$$N_v(\text{follicle subpopulations}) = \left[ \frac{\sum Q}{(a/f \times \sum P \times h)} \right] \times t/BA.$$

In this formula,  $\sum Q$  is the number of the follicle coming into in dissector height,  $\sum P$  denotes the total counted frames per mice for follicles in all microscopic fields, and  $h$  shows the height dissector measured using the microcator,  $a/f$  represents the area of the frame,  $t$  is the mean actual thickness of the section calculated by the microcator, and  $BA$  stands for the block advance of the microtome. The thickness of the ovary section was calculated in the whole microscopic fields of view with uniform random sampling from each ovary section. The total number of follicles was assessed by multiplying the numerical density by  $V(\text{ovary})$ .<sup>17</sup>

#### Statistical analysis

The data were statistically analyzed using IBM SPSS 16.0 (SPSS Inc., Chicago, IL, USA). All data were reported as the mean  $\pm$  standard deviation (SD). Kolmogorov-Smirnov test was utilized to evaluate the normality of the data. The samples were compared using one-way ANOVA with a post-hoc Tukey test. Before-after comparisons were evaluated by paired T-test. Comparison between two groups was carried out by independent T-test. Tests were performed within a 95% confidence interval at the significant level of  $p < 0.05$ .

## Results

### Estrus Cyclicity determination

Vaginal cytology in letrozole-receiving mice showed a diestrus phase continuity. Other treatment groups, however, exhibited the estrous cycle was regular.

### Weight

The weight of the mice in the first and third weeks is listed in Table 1. In the third week, the weight of PCOS mice was significantly higher than the control group (0.001). Metformin (0.001) and NAC (0.001) managed to correct PCOS-induced weight gain.

### Testosterone Serum level

Testosterone levels of the PCOS group were higher than the control group. Compared to PCOS, testosterone levels of other groups were lower.

### Uterine and ovarian stereological characteristics

#### Uterine weight

Uterine weight was significantly higher in the PCOS group. (PCOS - control groups (0.009), PCOS - metformin (0.03) and PCOS-NAC (0.008)).

#### Uterine volumetric results

The endometrial volume was higher in PCOS group (control - PCOS (0.008), PCOS - metformin (0.01), NAC - PCOS group (0.02)).

The myometrial volume was significantly higher in PCOS mice (PCOS-control (0.01), PCOS-metformin (0.04), and NAC-PCOS (0.01)).

The perimetrium volume was not significant in any group.

Endometrium sub structures volumetric results:

The volume of the endometrial lumen was not significantly changed in any group.

The volume of glands was higher in the PCOS group [PCOS-metformin (0.007), PCOS-control (0.004), and NAC-PCOS (0.01)].

The epithelial volume was higher in the PCOS group [PCOS-control (0.001), PCOS-metformin (0.003), NAC-PCOS groups (0.002)].

The stromal volume was significantly higher in the PCOS group [PCOS-control (0.005), PCOS-metformin (0.005), and PCOS-NAC (0.004)].

The volume of endometrial vessels was significantly lower in PCOS mice and higher in the metformin and NAC group [PCOS-control (0.01), PCOS-metformin (0.0001), metformin-control (0.01), NAC-PCOS group (0.001), and NAC-control (0.001)].

Type, number, and volume of endometrial gland:

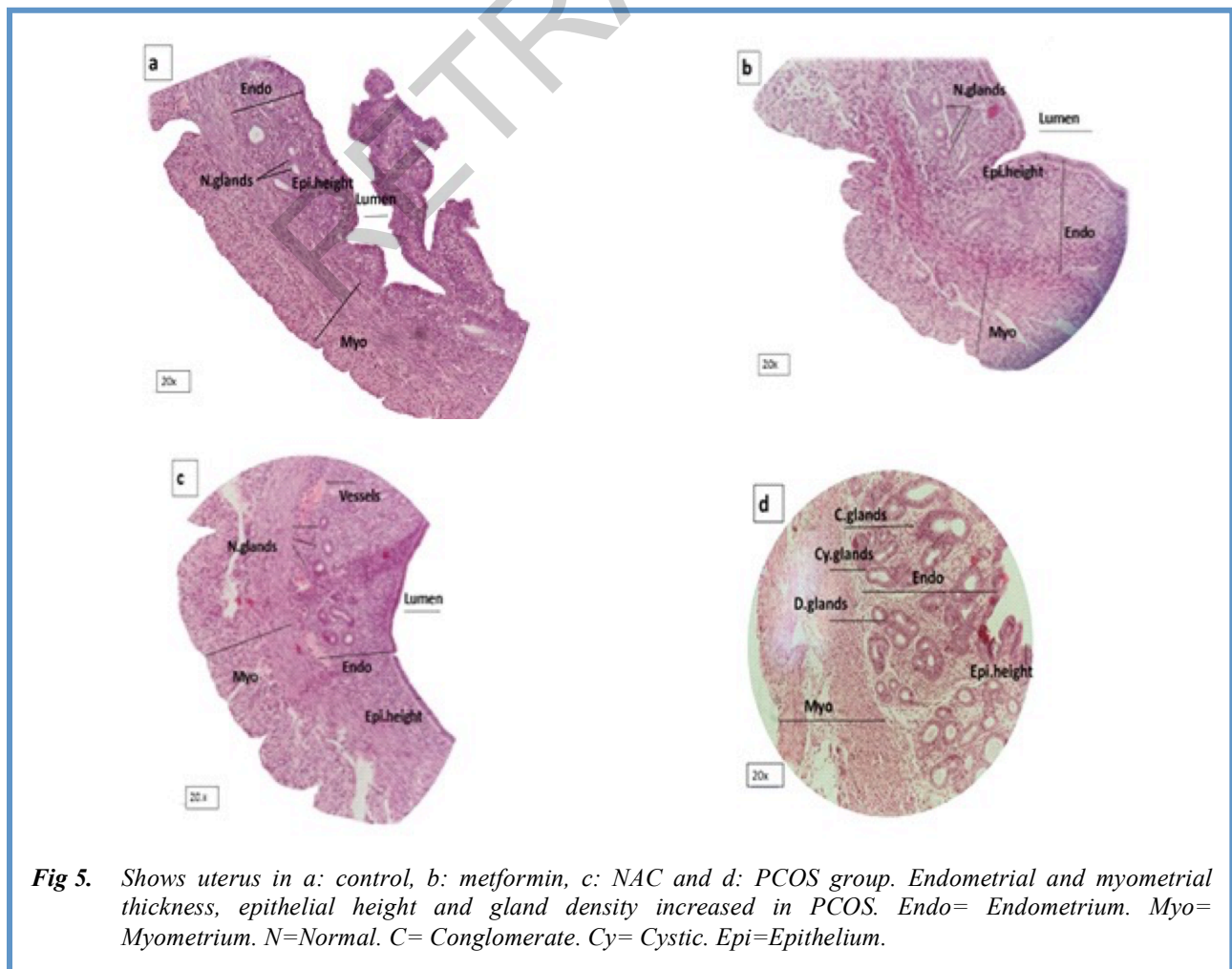
Total endometrial gland number was higher in PCOS group [PCOS-control (0.001), PCOS-metformin (0.001), PCOS-NAC (0.001)].

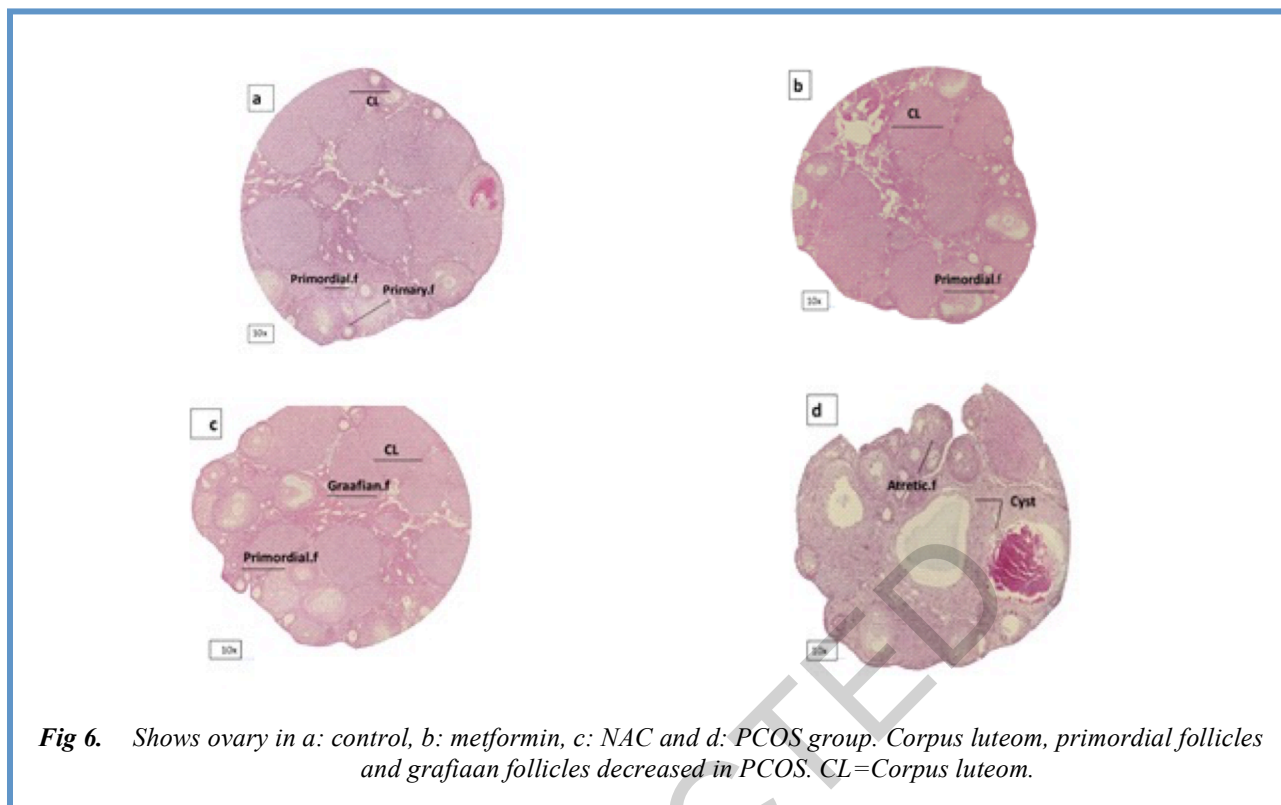
Number of normal endometrial glands was lower in PCOS group [PCOS-control (0.04), metformin-PCOS (0.006), NAC-PCOS (0.006)]. The number of endometrial cystic glands showed no significant change in none of the studied groups. PCOS group possessed more daughter endometrial glands [control-PCOS (0.0001), metformin-PCOS (0.0001), NAC-PCOS groups (0.0001)].

The number of endometrial conglomerate glands was higher in the PCOS group [PCOS-control (0.0001), PCOS-metformin (0.0001), and NAC - PCOS (0.0001)].

The volume of normal glands was lower in PCOS mice [control-PCOS (0.005), metformin-PCOS (0.003), PCOS-NAC (0.002)]. The volume of endometrial cystic glands was not significant in any group. The volume of endometrial daughter glands was higher in the PCOS group [control-PCOS (0.0001), metformin-PCOS (0.0001), and NAC-PCOS groups (0.0001)]. The volume of endometrial conglomerate glands was higher in the PCOS mice [control-PCOS (0.0001), metformin-PCOS (0.0001), NAC-PCOS (0.0001)].

Endometrial-myometrial thickness





The endometrial thickness was higher in the PCOS group [control-PCOS (0.0001), metformin-PCOS (0.0001), and NAC-PCOS (0.0001)]. The myometrial thickness was significantly higher in the PCOS mice [control-PCOS (0.02), metformin-PCOS (0.03), and NAC-PCOS (0.01)].

#### Endometrial vessel length

The endometrial vessels length was shorter in the PCOS mice and longer in the metformin and NAC treatment groups [control-PCOS (0.02), metformin-PCOS (0.001), control-metformin (0.003), NAC-control (0.06), and NAC-PCOS (0.0001)].

#### Volumetric and follicular count results:

The ovarian volume was higher in the PCOS group [control-PCOS (0.0001), metformin-PCOS (0.0001), and NAC-PCOS groups (0.0001)]. The cortical volume was significantly higher in the ovary of the PCOS subjects (control-PCOS (0.0001), metformin-PCOS (0.0001), and NAC - PCOS (0.0001)).

The difference in the medullary volume was significant between control-PCOS (0.0002), metformin-PCOS (0.0001), and NAC-PCOS (0.008).

Number of primordial follicles was lower in PCOS ovaries [control-PCOS (0.0001), metformin-PCOS (0.0001), and NAC-PCOS (0.01)]. Number of primary follicles was significantly higher in PCOS mice [control-PCOS (0.0001), metformin-PCOS (0.0001), and NAC-PCOS (0.0002)]. Number of secondary follicles was higher in the PCOS group [control-PCOS (0.0001), metformin-PCOS (0.0001), NAC-PCOS

(0.0006)]. Number of Graafian follicles was lower in the PCOS ovaries [control-PCOS (0.02), metformin-PCOS (0.02), and NAC-PCOS (0.02)]. The number of atretic follicles was significantly higher in the PCOS group [control-PCOS (0.04), metformin-PCOS (0.04), and NAC-PCOS (0.04)]. The number of ovarian cysts was significantly higher in the PCOS ovaries [control-PCOS (0.0006), metformin-PCOS (0.0006), NAC-PCOS groups (0.0002)]. The number of corpus luteum was lower in the PCOS group (control-PCOS (0.0001), metformin-PCOS (0.0001), and NAC-PCOS (0.008)). Weight, serum testosterone, and continuous diestrus in the vaginal smear of the PCOS group at the 4th week were the same as the first week ( $p=0.2$ ) and were considered as PCOS range.

#### Discussion

PCOS is a reproductive-metabolic disorder whose relationship with obesity has been well identified.<sup>29</sup> Hyperandrogenism is an early predictor of metabolic disorders in PCOS. Studies on twins showed that genetic and environmental factors such as prenatal exposure to too much androgen can play an important role in the development of this disorder.<sup>30</sup> Other causes of weight gain include increased leptin, abdominal fat, elevated fasting glucose, and insulin resistance.<sup>31</sup> PCOS mice of this study also exhibited estrous acyclicity and continuous diestrus phase in vaginal cytology. Studies indicated that animal models of PCOS are associated with persistent diestrus phase; some showed irregular sexual cycles depending on the type of

**Table 1.** Comparison of mice weight in control, PCOS, metformin group, treatment with N-acetylcysteine and its control in the first and third weeks.

Groups	Mean ± SD mice weight first week (g)	Mean ± SD mice weight first week (g)	p.value
Control	26.82±1.01	26.47±0.80	0.99
PCOS	28.06±2.41	35.47 ±1.70	0.0001*
Metformin	27±2.62	25.35 ± 1.36	0.006
p.value	0.2	0.001	
NAC	27.18 ±1.23	26.65 ±1.5	0.1
Control. NAC	27.71±1.21	27.53±1.32	0.72
P. value	0.05	0.2	

**Table 2.** Comparison of number of endometrial glands in control group, PCOS metformin, NAC, and NAC control.

Groups	normal glands	cystic glands	daughter glands	conglomerate glands
Control	(%68) 10.20±5.1	(%18.66) 2.80±0.44	(%8) 1.2±0.44	(%5.3) 0.8±0.44
PCOS	(%11.51) 4.4±2.30	(%8.42) 3.20±2.1	(%38) 14.44±3.97	(%42.63) 16.20±2.28
Metformin	(%66.31) 12.60±1.67	(%20) 3.80±1.30	(%8.42) 1.60±0.89	(%11.11) 1±0.70
p.value	0.07	0.5	0.001*	0.0001*
NAC	(%72.63) 13.80±3.11	(%14.73) 2.80±1.09	(%8.42) 1.60±1.14	(%6.31) 1.2±0.4
Control.NAC	(%22.10) 14.20±2.28	(%12.63) 2.40±1.5	(%7.36) 1.40±1.5	(%6.8) 1.3±0.70
p.value	0.8	0.6	0.8	0.9

**Table 3.** Comparison of ovarian follicular count in control, PCOS, metformin and NAC control group s.

Groups	Primordial-F	Primary-F	Secondary-F	Graafian-F	Atretic-F	Cystic-F	Corpus luteum
Control	191.8±48.08	126.7±33.61	16.10±4.39	54.11±17.34	17.34±6.36	22.49±8.32	109.9±26.19
PCOS	54.83±15.16	355.4±83.36	101.3±34.83	22.80±15.16	90.51±84.40	322.6±156	32.85±12.82
Metformin	208.14±34.27	101.4±26.29	15.52±4.54	53.09±14.01	9.83±4.62	27.27±9.17	120±11.61
p.value	0.0001*	0.0001*	0.0001*	0.01*	0.04*	0.0002*	0.0001*
NAC	196.6±102.6	86.35±37.40	14.17±5.56	53.49±20.03	6.22±4.26	14.49±7.14	153±75.99
NAC.Control	184.1±68.97	97.26±47.28	16.10±5.42	52.51±10.61	11.96±6.45	30.34±7.52	113.4±38.76
P.value	0.8	0.6	0.5	0.9	0.1	0.2	0.3

medication, duration, and androgen level. Manneras et al. showed that the dihydrotestosterone induced PCOS animal models are associated with the estrus cycle irregularities instead of continuous diestrus.<sup>32</sup> Histological observations suggest folliculogenesis disorder as a reason for the altered sexual cycle.<sup>33</sup> The results of a stereological study on letrozole-induced PCOS rats showed a significant rise in total ovarian volume, cortico-medullary volume, and the number of atretic follicles and ovarian cysts.<sup>20</sup> However, ovarian size decreased in another study that used estradiol valerate instead of letrozole.<sup>34</sup> This difference may be due to the type of medication used to induce PCOS as

well as its dose, which ultimately affected the serum level of testosterone in the blood.

For example, Manneras et al.<sup>32</sup> applied DHT to induce PCOS, which resulted in a decrement in ovarian weight and volume. The number of secondary follicles was also reduced in contrast to this study.<sup>32</sup>

Some studies have suggested that despite general insulin resistance, the ovaries remained sensitive to insulin responded to hyperinsulinemia by getting enlarged and producing more androgens, which can explain the increase in ovarian volume in the PCOS group.<sup>35</sup> By stimulating ovarian cell proliferation, hyperinsulinemia can ultimately increase ovarian volume and size, as well as the development of ovarian cysts.<sup>36</sup> hyperinsulinemia

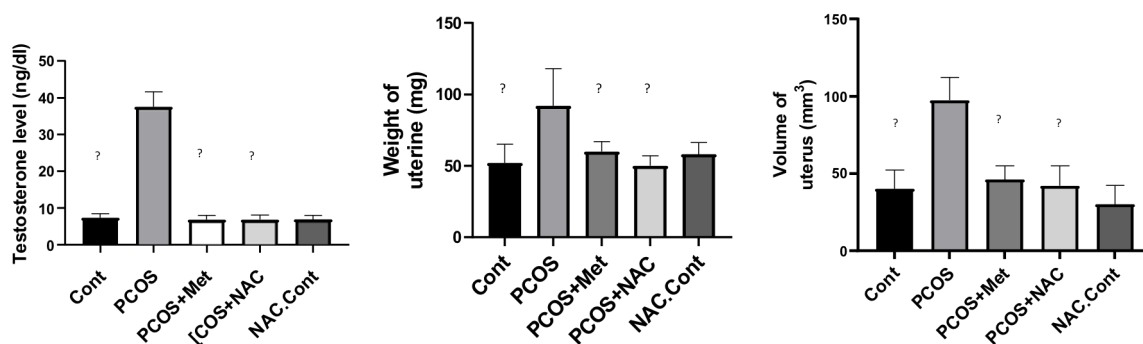


**Fig 7.** The level of serum testosterone, uterine weight, uterine volume. Data are the mean  $\pm$  SEM. Statistical analyses were performed by ANOVA followed by Tukey's test for multiple comparisons. Means without a common letter are significantly different ( $P < 0.05$ ).

can increase the production of androgens from theca cells and worsen the condition. On the other hand, there is a strong association between high androgen and proinflammatory cytokines called TNF- $\alpha$ . This cytokine can play an important role in the pathological increase of ovarian volume, follicular atresia and premature ovarian failure.<sup>37</sup>

Pathological examination of PCOS-affected ovaries showed an increment in atretic follicles, ovarian cysts, decreased corpus luteum, and estrus cycle irregularities. Decrease in primary follicles and increase in primary, secondary, and atretic follicles indicate cessation of folliculogenesis.<sup>38</sup> Some primary and secondary follicles become enlarged, and some become atretic. On the other hand, increasing the level of AMH in PCOS increases the number of secondary follicles. Elevated AMH levels play an important role in follicular arrest by inhibiting aromatase and reducing FSH activity and ultimately impairing dominant follicle selection.<sup>39,40</sup>

Decreased corpus luteum occurs due to the absence of ovulation. Decreased estradiol levels (as a result of inhibition of testosterone aromatization to estradiol) cause apoptosis and damage to the genetic material of the oocyte due to oxidative stress and thus increase follicular atresia.<sup>41</sup> Another reason for the increase in follicular atresia is the sudden lack of FSH surge and decrease in follicular sensitivity to FSH, which is due to the antagonistic effect of androgens on FSH and is the most important factor in stopping follicular growth.<sup>42</sup>

Ovarian exposure to large amounts of testosterone, before puberty, can enhance the number of primitive follicles.<sup>43</sup> After puberty, an increase in testosterone will cause the loss of primordial follicles, as happened in the present study.<sup>44</sup> Franks et al. stated that PCOS is a condition that prevents the selection of dominant follicles. Many secondary follicles accumulate in the ovary due to the effect of androgens on secondary follicles development arrest.<sup>45</sup>

The results of a study conducted on DHEA-induced PCOS mice showed an increment in the average of the endometrium, myometrium thickness, endometrial

epithelium, and endometrial glands.<sup>46</sup> PCOS can dramatically influence the uterus of affected women, eventually leading to an increased risk of hyperplasia and endometrial cancer.<sup>47</sup>

An increase of androgens through androgen receptors leads to epithelial cell proliferation and increased glandular formation (by increasing glandular epithelial proliferation).<sup>48</sup> Bracho et al. (2019) reported the association of uterine change in PCOS models with increased uterine weight, luminal epithelium height, gland size and density, and uterine thickness.<sup>49</sup> These changes can be assigned to uterine atrophy in some animal models. For example, the results of a study on DHT-induced PCOS rats models showed lower ovarian and uterine weight compared to the controls.<sup>50,51</sup> However, these differences appear to be due to the different effects of androgens on different components of the uterus. Selected non-aromatized androgen receptor agonists specifically increase the myometrial thickness of rodents with less effect on the endometrium. While testosterone increases the weight of the uterus, it enhances the thickness of the endometrium, myometrium, causing a gradual trophic effect on the rodent's uterus.<sup>48</sup> Uterine tissue responds to insulin in addition to steroid hormones. Insulin can inhibit endometrial stromal differentiation (decidualization).<sup>50</sup> PTEN, a tumor suppressor which is reduced in many cancers such as endometrial cancer, also showed a decrease in the uterus of PCOS mice, leading to elevated cellular mitosis.<sup>51</sup>

Increased androgens can cause proinflammation oxidative stress and lead to the development of precancerous components.<sup>52-54</sup> A limited number of studies have addressed the length of endometrial vessels in mice with PCOS, their results, however, show that PCOS patients who lack ovulation also have changes in the uterine vascularity. The pulsatility and resistance of blood vessels, which are inversely related to blood flow, increase in PCOS patients, which can reduce endometrial receptivity.<sup>52</sup> Hyperandrogenism has a significant negative effect on endometrial blood flow in

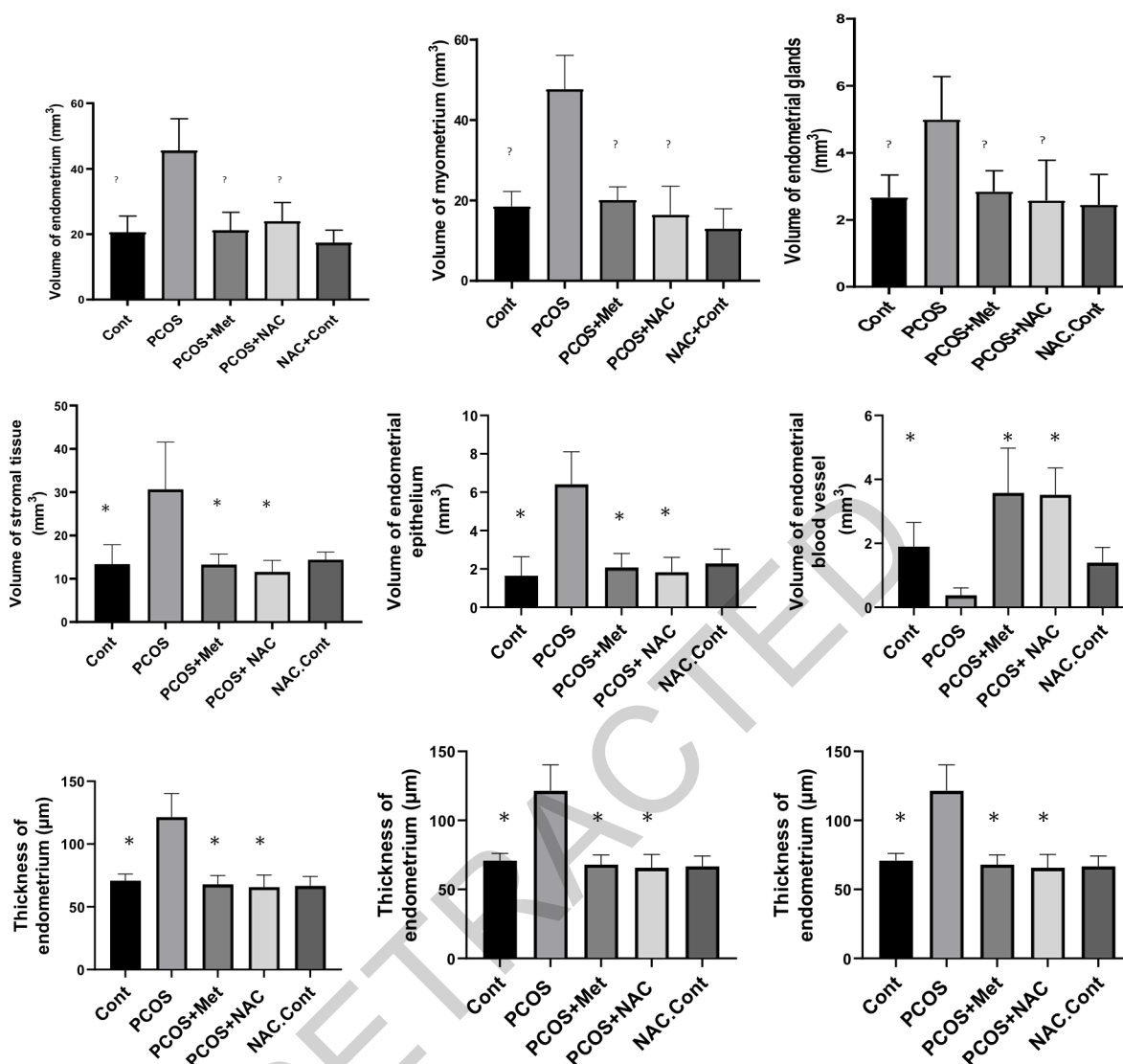


**Fig 8.** The endometrial volume, myometrial volume, gland volume, stromal volume, epithelial volume, endometrial blood vessel volume, endometrial thickness, myometrial thickness, endometrial vessel length. Data are the mean  $\pm$  SEM. Statistical analyses were performed by ANOVA followed by Tukey's test for multiple comparisons. Means without a common letter are significantly different ( $P < 0.05$ ).

PCOS. There is a direct statistical relationship between vascular resistance and serum testosterone.<sup>53</sup> Androgen is a vasoconstrictor that reduces uterine blood flow. On the other hand, blood flow in the endometrium is reduced in PCOS by decreasing estrogen (a factor that controls angiogenesis in the endometrium and uterine smooth muscle) and increasing endothelin-1 (a peptide that is secreted from the muscular part of the arteries when the arteries are narrowed).<sup>54</sup>

In the present study, metformin and NAC could significantly treat hyperandrogenism and weight gain in PCOS mice. They also regularized the estrus cycle. Results did not show a significant difference between NAC or metformin. Metformin can significantly reduce LH, LH/FSH ratio and decrease testosterone levels in

PCOS.<sup>55</sup> Metformin, however, inhibits the release of androstenedione and testosterone from ovarian theca cells.<sup>56</sup> By affecting adipose tissue, metformin inhibits lipogenesis and helps to lose weight. By reducing androgen levels, correcting hormonal profiles, and increasing insulin sensitivity, BMI decreased, ovulation takes place, and the estrus cycle gets regulated.<sup>57</sup> NAC is a safe antioxidant with a very high lethal dose. Animal studies show that this drug is neither teratogenic nor mutagenic. Unlike metformin, it has no side effects and is well tolerated by the patient. NAC increases insulin production by acting on pancreatic cells and insulin receptors in erythrocyte cells. NAC also increases environmental sensitivity to insulin and thereby lowers androgen levels and is used as an

ovulation stimulant with other drugs such as clomiphene

reduction is NAC-mediated ovulation resumption and

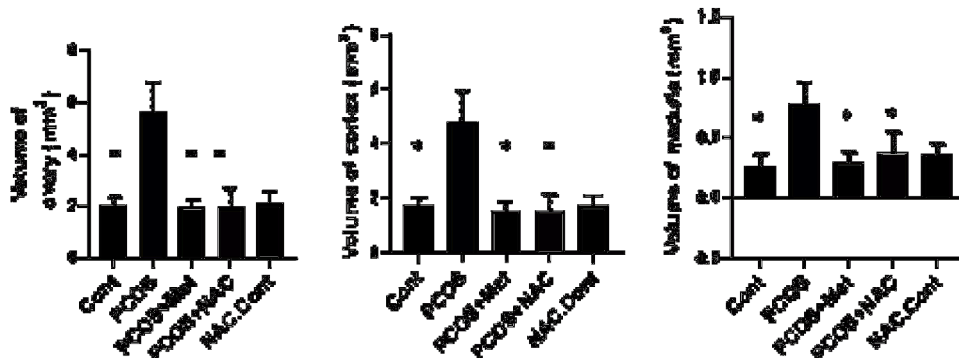


**Fig 9.** Ovarian volume, cortical volume, medullary volume. Data are the mean  $\pm$  SEM. Statistical analyses were performed by ANOVA followed by Tukey's test for multiple comparisons. Means without a common letter are significantly different ( $P < 0.05$ ).

citrate.<sup>58</sup>

A study showed that NAC consumption can reduce testosterone and LH levels.<sup>59</sup> Few studies addressed weight loss and estrus cycle regulation by NAC, however, it seems that the most important mechanism for weight loss and estrus cycle regulation in the present study is androgen reduction.

In the present study, both metformin and NAC managed to reduce total ovarian and cortico-medullary volume. The number of corpus luteum, primordial and graafian follicles increased; while the number of primary, secondary, atretic follicles, and ovarian cysts decreased. The results showed no significant difference between metformin and NAC concerning ovarian parameters. A significant relationship has been observed between the reduction of secondary follicles and the reduction of AMH levels in the metformin-treated group as the reduction of AMH levels is associated with increased aromatase activity and estradiol production that support folliculogenesis.<sup>60</sup> Metformin influences cumulus and theca cells by increasing the activity of enzymes involved in the production of steroid hormones such as estradiol and progesterone. Progesterone plays a decisive role in follicular maturation and resumption of meiosis in oocytes, ovulation, and the elevation of the corpus luteum.<sup>61</sup>

NAC causes spontaneous ovulation and enhances the corpus luteum, which is consistent with the results of the present study. NAC can also increment the dominant follicles, mainly by reducing the level of extracellular cystine, increasing glutathione activity, and finally reducing free radicals and apoptosis.<sup>62</sup> Another possible mechanism by which NAC augment dominant follicles involves an increase in estradiol and progesterone levels.<sup>63</sup> NAC is a powerful antioxidant that protects the follicles from atresia by its anti-apoptotic mechanism.<sup>64</sup> It seems that mechanism underlying ovarian volume

reduction of large ovarian cysts.

The results of this study showed a decline in uterine weight and volume and height of endometrium, myometrium, and endometrial components (stroma, glands, epithelium) in both the metformin and NAC groups to the level of the control group. Vascular volume and vessel length were increased compared to control and PCOS groups. The number of normal glands also exhibited a rise. The number of daughter and conglomerate glands decreased while lumen volume, perimeter volume, and number of cystic glands remained unchanged.

Metformin changes the morphology of uterine cells by inhibiting testosterone and androgen receptor levels (through acting on androgen receptors and epithelial growth factor, inhibiting insulin resistance, and reducing uterine inflammation). By reducing androgen receptors expression, the hyperplastic endometrium could be corrected.<sup>65</sup> Metformin can also inhibit the neoplastic growth of uterine cells by controlling glucose metabolism, increasing insulin sensitivity, and altering intracellular signaling pathways. Metformin has shown antimitogenic effects that can inhibit proliferation and differentiation in endometrial cells and reduce its thickness.<sup>66</sup> A study showed that metformin reduces luminal epithelial height, gland density, and endometrial thickness.<sup>67</sup> Metformin can directly increase vascular endothelial growth factor (VEGF) production and increase angiogenesis, blood flow and endometrial receptivity.<sup>68</sup> The results of a study showed an increment in the number of normal and cystic glands in the metformin group compared to PCOS while daughter and conglomerate glands showed a decline.<sup>69</sup>

NAC enhanced estradiol levels and decreased androgen. The results of a study showed that the use of NAC reduced the neoplastic activity of cells by affecting the luminal epithelium and glands exposure to radiation, making them like the control group.<sup>70</sup> NAC can

accelerate the process of angiogenesis by controlling VEGF.<sup>71</sup> Based on the limited number of studies on the effect of NAC on uterine tissue, it seems that the most important mechanisms of action of NAC involve reducing androgens and free radicals as well as increasing insulin sensitivity.

In conclusion, this study investigated the stereological and pathological features of PCOS mice and their treatment with metformin and NAC. Given the prevalence of PCOS and its impact on fertility, the use of non-invasive methods is of crucial prominence. As a harmless drug, NAC can control and treat pathological parameters for the treatment of women with PCOS.

### List of acronyms

GC - glucocorticoid

HPA - hypothalamic-pituitary-adrenal

IV - intravenous

oi – orthogonal intercepts

PCA - intravenous patient-controlled analgesia

POVN - postoperative nausea and vomiting

VAS - visual analog scale

### Contributions of Authors

GAA, AME and FNA: conception and design of the study, acquisition, analysis and interpretation of data, wrote the manuscript, performed literature review, article drafting and revision, reviewed and edited the manuscript critically, all authors approved the final version.

### Acknowledgments

This work was performed at the Histomorphometry and Stereology Research Center, Shiraz University of Medical Sciences, Shiraz, Iran. This study is part of the Ph.D. thesis (19333) written by Bahare Rafiee.

### Funding

This study was funded by Shiraz University of Medical Sciences.

### Conflict of Interest

The authors declare no conflict of interests.

### Ethical Publication Statement

We confirm that we have read the Journal's position on issues involved in ethical publication and affirm that this report is consistent with those guidelines.

### Corresponding Author

Soghra Bahmanpour, Professor of Anatomy, School of Medicine, Shiraz University of Medical Sciences, Shiraz, Iran

ORCID iD: 0000-0001-9598-2796

E-mail: [bahmans@sums.ac.ir](mailto:bahmans@sums.ac.ir)

E-mails and ORCID iD of co-authors

Bahare Rafiee: [b.rafaee@gmail.com](mailto:b.rafaee@gmail.com)

ORCID iD: 0000-0002-5890-0023

Saied Karbalay-doust: [karbalas@sums.ac.ir](mailto:karbalas@sums.ac.ir)

ORCID iD: 0000-0001-5782-7402

Seyed Mohammad Bagher Tabei: [tabeismb@sums.ac.ir](mailto:tabeismb@sums.ac.ir)

ORCID iD: 0000-0001-9923-6969

Negar Azarpira: [nagarazarpira@gmail.com](mailto:nagarazarpira@gmail.com)

ORCID iD: 0000-0002-5549-0057

Sanaz Alaei: [sanaz620@gmail.com](mailto:sanaz620@gmail.com)

ORCID iD: 0000-0003-4490-8830

Parvin Lohrasbi: [parvin.lohrasbi156@gmail.com](mailto:parvin.lohrasbi156@gmail.com)

ORCID iD: 0000-0003-3460-4729

### References

1. Escobar-Morreale HF. Polycystic ovary syndrome: definition, aetiology, diagnosis and treatment. *Nature Reviews Endocrinology*. 2018;14(5):270-84. doi: 10.1038/nrendo.2018.24. Epub 2018 Mar 23.
2. Azziz R, Carmina E, Chen Z, Dunaif A, Laven JS, Legro RS, et al. Polycystic ovary syndrome. *Nature reviews Disease primers*. 2016;2(1):1-18. doi: 10.1038/nrdp.2016.57.
3. Amato G, Conte M, Mazziotti G, Lalli E, Vitolo G, Tucker AT, et al. Serum and follicular fluid cytokines in polycystic ovary syndrome during stimulated cycles. *Obstetrics & Gynecology*. 2003;101(6):1177-82. doi: 10.1016/s0029-7844(03)00233-3.
4. Indhavivadhana S, Rattanachaiyanont M, Wongwananuruk T, Techatraisak K, Tanmahasamut P, Dangrat C. Brief communication (Original). Hyperandrogenemia is associated with thin endometrium in reproductive-aged Thai women with polycystic ovary syndrome. *Asian Biomedicine*. 2013;7(4):545-51.
5. Kitaya K, Matsubayashi H, Yamaguchi K, Nishiyama R, Takaya Y, Ishikawa T, et al. Chronic endometritis: potential cause of infertility and obstetric and neonatal complications. *American Journal of Reproductive Immunology*. 2016;75(1):13-22. doi: 10.1111/aji.12438. Epub 2015 Oct 18.
6. Komal F, Khan MK, Imran M, Ahmad MH, Anwar H, Ashfaq UA, et al. Impact of different omega-3 fatty acid sources on lipid, hormonal, blood glucose, weight gain and histopathological damages profile in PCOS rat model. *Journal of Translational Medicine*. 2020;18(1):1-11. doi: 10.1186/s12967-020-02519-1.
7. Huang Y, Yu Y, Gao J, Li R, Zhang C, Zhao H, et al. Impaired oocyte quality induced by dehydroepiandrosterone is partially rescued by metformin treatment. *PloS one*. 2015;10(3):e0122370. doi: 10.1371/journal.pone.0122370.
8. Di Pietro M, Parborell F, Irusta G, Pascuali N, Bas D, Bianchi MS, et al. Metformin regulates ovarian angiogenesis and follicular development in a female polycystic ovary syndrome rat model.

- Endocrinology. 2015;156(4):1453-63. doi: 10.1210/en.2014-1765. Epub 2015 Jan 15.
9. The effect of L-carnitine and metformin on histomorphology characteristics of uterus in mice with polycystic ovary. *Biharean Biologist*. 2020;14(1).
  10. Zhai J, Yao G-D, Wang J-Y, Yang Q-L, Wu L, Chang Z-Y, et al. Metformin regulates key microRNAs to improve endometrial receptivity through increasing implantation marker gene expression in patients with PCOS undergoing IVF/ICSI. *Reproductive Sciences*. 2019;26(11):1439-48. doi: 10.1177/1933719118820466. Epub 2019 Jan 1.
  11. Sandhu JK, Waqar A, Jain A, Joseph C, Srivastava K, Ochuba O, Alkayyali T, Ruo SW, Poudel S. Oxidative Stress in Polycystic Ovarian Syndrome and the Effect of Antioxidant N-Acetylcysteine on Ovulation and Pregnancy Rate. *Cureus*. 2021 Sep 11;13(9):e17887. doi: 10.7759/cureus.17887.
  12. Kamalipour F, Jalali H, Azamia M. Comparison the Effect of Metformin and Clomiphene Citrate on Sirtuin3 gene Expression in the Oocytes of Mice with Polycystic Ovary Syndrome. *Iranian Journal of Pharmaceutical Research: IJPR*. 2020;19(4):160. doi: 10.22037/ijpr.2020.113321.14236.
  13. Gonzalez G. Determining the stage of the estrous cycle in female mice by vaginal smear. *Cold Spring Harbor Protocols*. 2016;2016(8):pdb.prot094474. doi: 10.1101/pdb.prot094474
  14. Mühlfeld C, Nyengaard JR, Mayhew TM. A review of state-of-the-art stereology for better quantitative 3D morphology in cardiac research. *Cardiovascular Pathology*. 2010;19(2):65-82. doi: 10.1016/j.carpath.2008.10.015. Epub 2009 Jan 14.
  15. Sá SI, Maia J, Bhowmick N, Silva SM, Silva A, Correia-da-Silva G, et al. Uterine histopathological changes induced by acute administration of tamoxifen and its modulation by sex steroid hormones. *Toxicology and Applied Pharmacology*. 2019;363:88-97. doi: 10.1016/j.taap.2018.11.015. Epub 2018 Nov 29.
  16. Dorph Petersen KA, Nyengaard J, Gundersen H. Tissue shrinkage and unbiased stereological estimation of particle number and size. *Journal of microscopy*. 2001;204(3):232-46. doi: 10.1046/j.1365-2818.2001.00958.x.
  17. Pappalardo M, Vita R, Di Bari F, Le Donne M, Trimarchi F, Benvenga S. Gly972Arg of IRS-1 and Lys121Gln of PC-1 polymorphisms act in opposite way in polycystic ovary syndrome. *Journal of Endocrinological Investigation*. 2017;40(4):367-76. doi: 10.1007/s40618-016-0569-7. Epub 2016 Oct 26.
  18. Elia E, Vighi S, Lombardi E, Motta AB. Detrimental effects of hyperandrogenism on uterine functions. *International immunopharmacology*. 2008;8(13-14):1827-34. doi: 10.1016/j.intimp.2008.09.002. Epub 2008 Sep 24.
  19. Ferrando RE, Nyengaard JR, Hays SR, Fahy JV, Woodruff PG. Applying stereology to measure thickness of the basement membrane zone in bronchial biopsy specimens. *Journal of allergy and clinical immunology*. 2003;112(6):1243-5. doi: 10.1016/j.jaci.2003.09.038.
  20. Noorafshan A, Ahmadi M, Mesbah S-F, Karbalay-Doust S. Stereological study of the effects of letrozole and estradiol valerate treatment on the ovary of rats. *Clinical and Experimental Reproductive Medicine*. 2013;40(3):115. doi: 10.5653/cerm.2013.40.3.115. Epub 2013 Sep 30.
  21. Karbalay-Doust S, Noorafshan A. Stereological estimation of ovarian oocyte volume, surface area and number: application on mice treated with nandrolone decanoate. *Folia histochemica et cytobiologica*. 2012;50(2):275-9. doi: 10.5603/fhc.2012.0037.
  22. Hayes MG, Urbanek M, Ehrmann DA, Armstrong LL, Lee JY, Sisk R, et al. Genome-wide association of polycystic ovary syndrome implicates alterations in gonadotropin secretion in European ancestry populations. *Nature communications*. 2015;6(1):1-13. doi: 10.1038/ncomms8502. Erratum in: *Nat Commun*. 2016;7:10762. Erratum in: *Nat Commun*. 2020 Apr 28;11(1):2158.
  23. Cassar S, Misso ML, Hopkins WG, Shaw CS, Teede HJ, Stepto NK. Insulin resistance in polycystic ovary syndrome: a systematic review and meta-analysis of euglycaemic-hyperinsulinaemic clamp studies. *Human reproduction*. 2016;31(11):2619-31. doi: 10.1093/humrep/dew243. Epub 2016 Oct 7.
  24. Walters K, Bertoldo M, Handelsman D. Evidence from animal models on the pathogenesis of PCOS. *Best Practice & Research Clinical Endocrinology & Metabolism*. 2018;32(3):271-81. doi: 10.1016/j.beem.2018.03.008. Epub 2018 Mar 31.
  25. Kauffman AS, Thackray VG, Ryan GE, Tolson KP, Glidewell-Kenney CA, Semaan SJ, et al. A novel letrozole model recapitulates both the reproductive and metabolic phenotypes of polycystic ovary syndrome in female mice. *Biology of reproduction*. 2015;93(3):69, 1-12. doi: 10.1095/biolreprod.115.131631. Epub 2015 Jul 22.
  26. Ryan GE, Malik S, Mellon PL. Antiandrogen treatment ameliorates reproductive and metabolic phenotypes in the letrozole-induced mouse model of PCOS. *Endocrinology*. 2018;159(4):1734-47. doi: 10.1210/en.2017-03218.
  27. Carmina E, Rosato F, Janni A. Extensive clinical experience. relative prevalence of different androgen excess disorders in 950 women referred

- because of clinical hyperandrogenism. 2006;91:2-6. doi: 10.1210/jc.2005-1457. Epub 2005 Nov 1.
28. Xu J, Dun J, Yang J, Zhang J, Lin Q, Huang M, et al. Letrozole rat model mimics human polycystic ovarian syndrome and changes in insulin signal pathways. *Medical science monitor: international medical journal of experimental and clinical research.* 2020;26:e923073-1. doi: 10.12659/MSM.923073.
  29. Dumesic DA, Oberfield SE, Stener-Victorin E, Marshall JC, Laven JS, Legro RS. Scientific statement on the diagnostic criteria, epidemiology, pathophysiology, and molecular genetics of polycystic ovary syndrome. *Endocrine reviews.* 2015;36(5):487-525. doi: 10.1210/er.2015-1018.
  30. Abbott DH, Bacha F. Ontogeny of polycystic ovary syndrome and insulin resistance in utero and early childhood. *Fertility and sterility.* 2013;100(1):2-11. doi: 10.1016/j.fertnstert.2013.05.023.
  31. Kelley ST, Skarra DV, Rivera AJ, Thackray VG. The gut microbiome is altered in a letrozole-induced mouse model of polycystic ovary syndrome. *PloS one.* 2016;11(1):e0146509. doi: 10.1371/journal.pone.0146509.
  32. Manneras L, Cajander S, Holmång A, Seleskovic Z, Lystig T, Lönn M, et al. A new rat model exhibiting both ovarian and metabolic characteristics of polycystic ovary syndrome. *Endocrinology.* 2007;148(8):3781-91. doi: 10.1210/en.2007-0168. Epub 2007 May 10.
  33. Rezvanfar MA, Shojaei Saadi HA, Gooshe M, Abdolghaffari AH, Baeeri M, Abdollahi M. Ovarian aging-like phenotype in the hyperandrogenism-induced murine model of polycystic ovary. *Oxidative medicine and cellular longevity.* 2014;2014. doi: 10.1155/2014/948951. Epub 2014 Feb 19.
  34. Brawer JR, Munoz M, Farookhi R. Development of the polycystic ovarian condition (PCO) in the estradiol valerate-treated rat. *Biology of reproduction.* 1986;35(3):647-55. doi: 10.1095/biolreprod35.3.647.
  35. Leeman L, Acharya U. The use of metformin in the management of polycystic ovary syndrome and associated anovulatory infertility: the current evidence. *Journal of Obstetrics and Gynaecology.* 2009;29(6):467-72. doi: 10.1080/01443610902829414.
  36. Poretsky L, Clemons J, Bogovich K. Hyperinsulinemia and human chorionic gonadotropin synergistically promote the growth of ovarian follicular cysts in rats. *Metabolism.* 1992;41(8):903-10. doi: 10.1016/0026-0495(92)90175-a.
  37. Kireev R, Tresguerres A, Garcia C, Borrás C, Ariznavarreta C, Vara E, et al. Hormonal regulation of pro-inflammatory and lipid peroxidation processes in liver of old ovariectomized female rats. *Biogerontology.* 2010;11(2):229-43. doi: 10.1007/s10522-009-9242-2. Epub 2009 Jul 26.
  38. Nabiuni M, Ghafurniyan H, Azarnia M, Karimzadeh L. The Effect of Green Tea Extract on Reproductive Improvement in Estradiol Valerate-Induced Polycystic Ovary Polycystic Ovarian Syndrome in Rat. *Iranian Journal of Pharmaceutical Research.* 2015;14(4):1215-23.
  39. Stracquadanio M, Ciotta L, Palumbo M. Relationship between serum anti-Mullerian hormone and intrafollicular AMH levels in PCOS women. *Gynecological Endocrinology.* 2018;34(3):223-8. doi: 10.1080/09513590.2017.1381838. Epub 2017 Sep 23.
  40. Matsuda F, Inoue N, Manabe N, Ohkura S. Follicular growth and atresia in mammalian ovaries: regulation by survival and death of granulosa cells. *Journal of Reproduction and Development.* 2012;58(1):44-50. doi: 10.1262/jrd.2011-012.
  41. Dumesic DA, Richards JS. Ontogeny of the ovary in polycystic ovary syndrome. *Fertility and sterility.* 2013;100(1):23-38.
  42. Agarwal SK, Judd HL, Magoffin DA. A mechanism for the suppression of estrogen production in polycystic ovary syndrome. *The Journal of Clinical Endocrinology & Metabolism.* 1996;81(10):3686-91. doi: 10.1210/jcem.81.10.8855823.
  43. Smith P, Steckler TL, Veiga-Lopez A, Padmanabhan V. Developmental programming: differential effects of prenatal testosterone and dihydrotestosterone on follicular recruitment, depletion of follicular reserve, and ovarian morphology in sheep. *Biology of reproduction.* 2009;80(4):726-36. doi: 10.1095/biolreprod.108.072801.
  44. Hillier SG, Ross GT. Effects of exogenous testosterone on ovarian weight, follicular morphology and intraovarian progesterone concentration in estrogen-primed hypophysectomized immature female rats. *Biology of Reproduction.* 1979;20(2):261-8. doi: 10.1095/biolreprod20.2.261.
  45. Franks S, Stark J, Hardy K. Follicle dynamics and anovulation in polycystic ovary syndrome. *Human reproduction update.* 2008;14(4):367-78. doi: 10.1093/humupd/dmn015. Epub 2008 May 22. Erratum in: *Hum Reprod Update.* 2008 Sep-Oct;14(5):539.
  46. Bandariyan E, Mogheiseh A, Ahmadi A. Study of Body Weight and Histomorphometry of Uterus in Experimentally Polycystic Ovary Syndrome Induced by Dehydroepiandrosterone in Mouse

- Models Treated with Lutein. *Journal of Veterinary Research*. 2021;76(2):242-9.
47. Giudice LC. Endometrium in PCOS: implantation and predisposition to endocrine CA. *Best practice & research Clinical endocrinology & metabolism*. 2006;20(2):235-44. doi: 10.1016/j.beem.2006.03.005.
  48. Simitsidellis I, Gibson DA, Cousins FL, Esnal-Zufiaurre A, Saunders PT. A role for androgens in epithelial proliferation and formation of glands in the mouse uterus. *Endocrinology*. 2016;157(5):2116-28. doi: 10.1210/en.2015-2032. Epub 2016 Mar 10.
  49. Bracho GS, Altamirano GA, Kass L, Luque EH, Bosquiazzo VL. Hyperandrogenism induces histo-architectural changes in the rat uterus. *Reproductive Sciences*. 2019;26(5):657-68. doi: 10.1177/1933719118783881. Epub 2018 Jun 21.
  50. Tas M, Kutuk MS, Serin IS, Ozgun MT, Oner G, Ozturk F. Comparison of antiproliferative effects of metformine and progesterone on estrogen-induced endometrial hyperplasia in rats. *Gynecological Endocrinology*. 2013;29(4):311-4. doi: 10.3109/09513590.2012.743010. Epub 2013 Jan 10.
  51. Virginia AM, Virginia TM, Laura K. Androgen receptor and uterine histoarchitecture in a PCOS rat model. *Molecular and Cellular Endocrinology*. 2020;518:110973. doi: 10.1016/j.mce.2020.110973. Epub 2020 Aug 8.
  52. Palomba S, Russo T, Orio Jr F, Falbo A, Manguso F, Cascella T, et al. Uterine effects of metformin administration in anovulatory women with polycystic ovary syndrome. *Human Reproduction*. 2006;21(2):457-65. doi: 10.1093/humrep/dei351.
  53. Lam P, Johnson I, Raine Fenning N. Endometrial blood flow is impaired in women with polycystic ovarian syndrome who are clinically hyperandrogenic. *Ultrasound in Obstetrics and Gynecology: The Official Journal of the International Society of Ultrasound in Obstetrics and Gynecology*. 2009;34(3):326-34. doi: 10.1002/uog.7314.
  54. Adali E, Kulusari A, Adali F, Yildizhan R, Kurdoglu M, Sahin HG. Doppler analysis of uterine perfusion and ovarian stromal blood flow in polycystic ovary syndrome. *International Journal of Gynecology & Obstetrics*. 2009;105(2):154-7. doi: 10.1016/j.ijgo.2008.12.023.
  55. Xie Y, Xiao L, Li S. Effects of Metformin on Reproductive, Endocrine, and Metabolic Characteristics of Female Offspring in a Rat Model of Letrozole-Induced Polycystic Ovarian Syndrome With Insulin Resistance. *Frontiers in Endocrinology*. 2021;12. doi: 10.3389/fendo.2021.701590.
  56. Lashen H. Role of metformin in the management of polycystic ovary syndrome. *Therapeutic advances in endocrinology and metabolism*. 2010;1(3):117-28. doi: 10.1177/2042018810380215.
  57. Stocker T. *Climate change 2013: the physical science basis: Working Group I contribution to the Fifth assessment report of the Intergovernmental Panel on Climate Change: Cambridge university press*; 2014.
  58. Badawy A, State O, Abdelgawad S. N-Acetyl cysteine and clomiphene citrate for induction of ovulation in polycystic ovary syndrome: a cross-over trial. *Acta obstetrica et gynecologica Scandinavica*. 2007;86(2):218-22. doi: 10.1080/00016340601090337. Erratum in: *Acta Obstet Gynecol Scand*. 2021 Jun 23.
  59. Wang L, Tang J, Zhou J, Zhu L, Tan F, Chen Y, et al. N-Acetylcysteine restores reproductive defects caused by Ggt1 deletion in mice. *Clinical and translational medicine*. 2021;11(8). doi: 10.1002/ctm2.510.
  60. Furat Rencber S, Kurnaz Ozbek S, Eraldemir C, Sezer Z, Kum T, Ceylan S, et al. Effect of resveratrol and metformin on ovarian reserve and ultrastructure in PCOS: an experimental study. *Journal of ovarian research*. 2018;11(1):1-16. doi: 10.1186/s13048-018-0427-7.
  61. Mansfield R, Galea R, Brincat M, Hole D, Mason H. Metformin has direct effects on human ovarian steroidogenesis. *Fertility and sterility*. 2003;79(4):956-62. doi: 10.1016/s0015-0282(02)04925-7.
  62. Maged AM, Elsawah H, Abdelhafez A, Bakry A, Mostafa WA. The adjuvant effect of metformin and N-acetylcysteine to clomiphene citrate in induction of ovulation in patients with Polycystic Ovary Syndrome. *Gynecological endocrinology*. 2015;31(8):635-8. doi: 10.3109/09513590.2015.1037269.
  63. Chang EY, Barbosa E, Paintlia M, Singh A, Singh I. The use of N-acetylcysteine for the prevention of hypertension in the reduced uterine perfusion pressure model for preeclampsia in Sprague-Dawley rats. *American journal of obstetrics and gynecology*. 2005;193(3):952-6. doi: 10.1016/j.ajog.2005.05.083.
  64. Salehpour S, Akbari Sene A, Saharkhiz N, Sohrabi MR, Moghimian F. N-acetylcysteine as an adjuvant to clomiphene citrate for successful induction of ovulation in infertile patients with polycystic ovary syndrome. *Journal of Obstetrics and Gynaecology Research*. 2012;38(9):1182-6. doi: 10.1111/j.1447-0756.2012.01844.x. Epub 2012 Apr 30.
  65. Ito-Yamaguchi A, Suganuma R, Kumagami A, Hashimoto S, Yoshida-Komiya H, Fujimori K. Effects of metformin on endocrine, metabolic

- milieus and endometrial expression of androgen receptor in patients with polycystic ovary syndrome. *Gynecological Endocrinology*. 2015;31(1):44-7. doi: 10.3109/09513590.2014.951321.
66. Bjørge T, Lukanova A, Jonsson H, Tretli S, Ulmer H, Manjer J, et al. Metabolic syndrome and breast cancer in the me-can (metabolic syndrome and cancer) project. *Cancer Epidemiology and Prevention Biomarkers*. 2010;19(7):1737-45. doi: 10.1158/1055-9965.EPI-10-0230.
67. Khalaf WM, Akl SA, Ramadan RR. Effect of Metformin on Endometrial Thickness and Subendometrial Flow Patterns in Anovulatory Patients with Polycystic Ovarian Syndrome. *Open Journal of Obstetrics and Gynecology*. 2018;8(14):1465.
68. Mahamed RR, Maganhin CC, Simões RS, de Jesus Simões M, Baracat EC, Soares Jr JM. Effects of metformin on the reproductive system of androgenized female rats. *Fertility and sterility*. 2011;95(4):1507-9. doi: 10.1016/j.fertnstert.2010.07.1093.
69. Elia EM, Belgorosky D, Faut M, Vighi S, Pustovrh C, Motta AB. The effects of metformin on uterine tissue of hyperandrogenized BALB/c mice. *Molecular human reproduction*. 2009;15(7):421-32. doi: 10.1093/molehr/gap033.
70. Gao W, Liang J-X, Ma C, Dong J-y, Yan Q. The protective effect of N-acetylcysteine on ionizing radiation induced ovarian failure and loss of ovarian reserve in female mouse. *Biomed Research International*. 2017;2017. doi: 10.1155/2017/4176170.
71. Licks F, Hartmann RM, Marques C, Schemitt E, Colares JR, do Couto Soares M, et al. N-acetylcysteine modulates angiogenesis and vasodilation in stomach such as DNA damage in blood of portal hypertensive rats. *World Journal of Gastroenterology*. 2015;21(43):12351. doi: 10.3748/wjg.v21.i43.12351.

Submission: February 13, 2022

Revision received: February 16, 2022

Accepted for publication: February 16, 2022

RETRACTED